

Validity using pump-probe pulses to determine **the** optical response of **niobate** crystals

Huimin Liu and Weiyi Jia

Department of Physics, University of Puerto Rico at Mayaguez  
Mayaguez, PR 00681, U.S.A.

## 1. INTRODUCTION

A variety of **niobate** crystals have found their places **in** nonlinear optical applications as **well** as in laser devices. **In** recent years much attention has been paid to study the **ultrafast** optical response in a variety of **photorefractive** crystals such as  $\text{KTa}_{1-x}\text{Nb}_x\text{O}_3$  and  $\text{KNbO}_3$  crystals<sup>1,2</sup>, glasses<sup>3</sup>, semiconductors and **polymers**<sup>5</sup> for applications in optical switching, information processing, optical computing, and all-optical device systems. Third-order optical nonlinearity is the most important property for realization of all-optical switching. Therefore experiments have been performed on the third order susceptibility using a variety of techniques such as the third-order harmonic generation, **EFISH** and degenerate four-wave **mixing**(DFWM). The latter has been conducted with a variety of pump **wavelengths** and with nanosecond, picosecond and **femtosecond** pulses.

**Niobate** crystals, such as potassium **niobate**  $\text{KNbO}_3$ , potassium tantalate **niobate** **KTN** family ( $\text{KTa}_{1-x}\text{Nb}_x\text{O}_3$ ), strontium barium **niobate** **SBN** ( $\text{Sr}_x\text{Ba}_{1-x}\text{Nb}_2\text{O}_6$ ) and potassium-sodium **niobate** **SBN** (**KNSBN**) are attractive due to their **photorefractive** properties for application in optical storage and processing. The pulsed probe experiments performed on these materials have suggested two types of time responses. These responses have been associated with an coherent response due to  $\chi^{(3)}$ , and a long lived component due to excited state population. Recent study of **DFWM** on  $\text{KNbO}_3$  and **KTN** family reveals that the long lived component of those crystals depends on the crystal orientation, A slowly decaying signal is observable when the grating vector  $\mathbf{K}_g$  is not perpendicular to the C-axis of those **photorefractive** crystals, otherwise the optical response signal would be **only** a narrow coherent peak with **FWHM** equal to **the** cross-correlation width of the write beam pulses. Based on this understanding, we study the **photodynamical** process of a variety of **niobate** crystals using **DFWM** in a  $\mathbf{K}_g \perp \text{C}$  geometry with a **ps-YAG:Nd** laser operating at **532nm**. However, the discrepancies in numerical estimations of  $\chi^{(3)}$  in these materials **and** other nonlinear optical **media**<sup>6</sup> have resulted in a number of **discussions**<sup>7,8</sup>. In order to better understand the **photodynamical** process of **niobate** crystals **after an** short pulse excitation we analyze the factors governing the coherent **signal** and present the **DFWM** spectra of **niobate** crystals.

## 2. EXPERIMENTAL

Host materials **SBN:61**, **KNaSBN:75** (potassium-sodium **SBN**) and mixed **KTN** ( $\text{KTa}_{1-x}\text{Nb}_x\text{O}_3$ ) **niobate** crystals with  $0 \leq x \leq 0.84$  and  $x=1$  were used in the experiment. The samples were poled along the C-axis, and cut with the C-axis along one of the **surfaces**. A **single 25 ps** pulse from a mode-locked, Q-switched **Nd:YAG** laser operating at 10 Hz was frequency doubled to  $\lambda=532 \text{ nm}$  and split into three pulses. These pulses were then spatially overlapped in the sample in the conventional backward propagating degenerate four-wave mixing geometry (see Fig. 1) with the counter propagating **beam** acting as the probe. The pulses were co-linearly polarized, with the pump beam/probe beam intensity ratio of 10:1. The scattered light was monitored by a **Molelectron** Joule meter and the output was stored in a computer. The **arrival** of the probe beam relative to the simultaneously arriving pump beams was controlled by a computer driven optical delay line, At the sample, the three beams **had** a nearly Gaussian spatial profile with a radius of  $250 \mu\text{m}$  for the pump beams and  $200 \mu\text{m}$  for the probe beam. The smaller probe beam radius reduces effects due to the **spatial** nature of the induced grating, particularly, effects arising from the Gaussian profile of the pump beams and variations due to pump beams crossing angle 20. The temporal and spatial overlap of the three beams at zero delay was determined by optimization

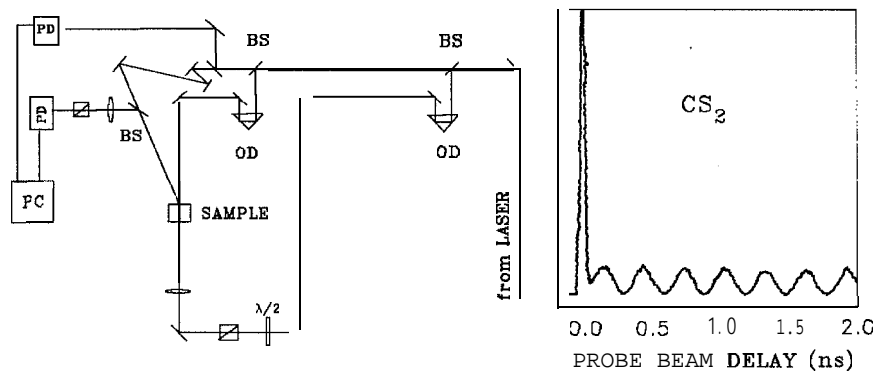


Fig. 1. Setup of DFWM experiment using  $\text{CS}_2$  as a standard,

of the instantaneous response signal from a  $\text{CS}_2$  sample. The value of  $2\theta$  was varied between  $3.20$ - $30.4^\circ$ . The polarization configuration of the four pulses including signal was (ssss). Further details of the laser system and optical delay lines are given in refs<sup>1</sup>.

### 3. DFWM spectra measurement

#### 3.1 DFWM spectra of host niobate crystals

Fig. 2 is the time-resolved DFWM spectrum obtained from  $\text{KNbO}_3$  crystal at the different orientation angle  $\phi$ , where  $\phi$  is the angle between  $\mathbf{K}_g$  and C-axis of the crystal. The spectrum of  $\phi=90^\circ$  also represents a common feature of instantaneous optical response signal of all poled (single domain) SBN and KSBN niobate crystals in the  $\mathbf{K}_g \perp \mathbf{C}$  geometry. This signal is associated with the third-order susceptibility of the material. It arises from fast, coherent processes. The FWHM of the signal is close to the autocorrelation width of three pulses, similar to that of a  $\text{CS}_2$  reference sample. No signal broadening is observed. The probe pulse, with intensity equal to 10% of the total laser intensity, was passed through an optical delay line, and was incident on the sample in a backward configuration. The sophisticated optical delay line used can reach an accuracy of 15 fs. When crystal is rotated or  $\phi$  decreases a slowly growing response signal observed starting from  $\phi=75^\circ$ . The spectrum is now composed of two signals: a sharp coherent signal with a peak at zero-delay, and a slowly rising signal component. The latter reaches its maximum intensity at  $\phi=0^\circ$  ( $\mathbf{K}_g // \mathbf{C}$ ). It reflects movement of the dynamic lattice due to creation of free-carriers. In the bright region of the grating produced by crossing two write-pulses inside the sample the carriers are created in the conduction band which consists of  $d\xi$  orbitals of Nb electrons, leaving behind holes in the valence band, which consists of  $p\pi$  orbitals of oxygen electrons. Under the action of intense internal electric field (single domain crystal) induced in the poling process along the C-axis, those free-carriers are caused to drift along the C-axis direction until trapped at  $\text{Nb}^{5+}$  sites, forming  $\text{Nb}^{4+}$  or so-called  $\text{Nb}^{4+}$ -hole small polarons<sup>9</sup>. They cause a temporal lattice distortion in C direction, and consequently alter the index of refraction along  $\mathbf{K}_g$  by a factor of  $(\cos\phi)$ . As  $\phi$  decreases to  $0^\circ$ , ( $\mathbf{K}_g // \mathbf{C}$  geometry), the coherent signal component is superimposed with the long lived slow component resulting in signal width completely masked. On the other hand, if the geometry is  $\mathbf{K}_g \perp \mathbf{C}$  or  $\phi=90^\circ$ , however, the resultant lattice distortion has no contribution along the  $\mathbf{K}_g$  direction, and thus no slow component could be observed.

The change in susceptibility  $\Delta\chi$  is related to  $A_n$ , and the change in the index of refraction is:

$$\Delta\chi = \Delta[(n + i kc/2\omega)^2 - 1] \quad (1)$$

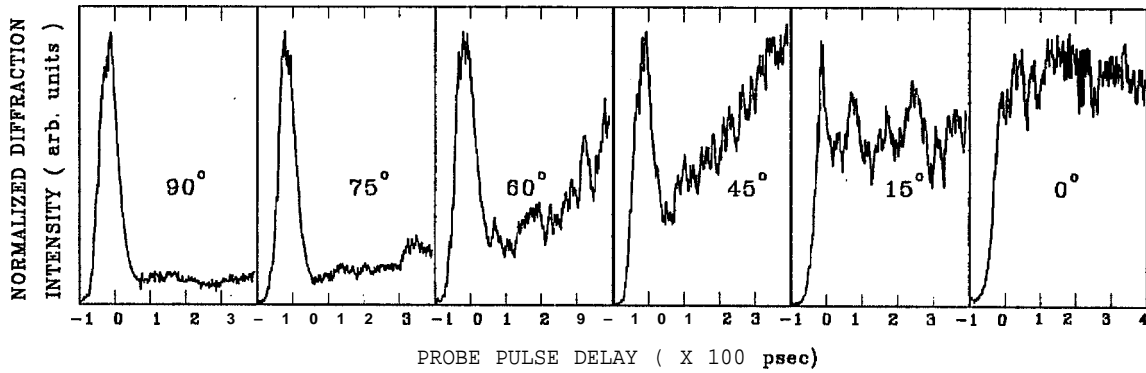


Figure 2. Time-resolved DFWM spectra of poled  $\text{KNbO}_3$  crystal, A narrow but intense signal at zero-delay of probe pulse represents the coherent optical response.

where  $\omega$  is the angular frequency of the write-beams.  $\Delta\chi$  is also a function of lattice distortion  $\Delta r$ , and is expressed as

$$\Delta\chi = \Delta N(3r^2/\xi + 1)\Delta r \cos\phi. \quad (2)$$

$N$  is the population density,  $r$ , the lattice constant of the crystal.  $\xi$  is a crystal dependent parameter,  $\Delta r$ , in principle, can be determined from luminescence measurements. Expression (2) reflects the crystal orientation dependence of the observed DFWM signal intensity. In Fig.2(c), where  $\mathbf{K}_g//C$  ( $\phi=0$ ), the change in susceptibility due to temporal lattice distortion reaches a maximum. This part of the contribution to susceptibility change is added to that due to the instantaneous grating. Since the space charge field is parallel to the C-axis and the lattice distortion occurred also along the C-axis, no time delay is needed for those carriers making a realignment, unlike what we have seen in figure 1(b).

### 3.2. ADJUSTMENT OF PUMP-PULSES IN DFWM

Under a good experimental condition the obtained DFWM spectrum of the  $\text{CS}_2$  standard shows a sharp coherent peak at zero time delay followed by an oscillating signal as shown in the insert of Figure 1. The relative delay between the two write pulses was carefully adjusted by monitoring the peak intensity of  $\text{CS}_2$  reference sample. A subtle variation in the relative delay was found to give a significant change in the obtained DFWM spectra. As shown in Fig. 2, the coherent signal of  $\text{CS}_2$  changes its profile as well as the peak intensity if the relative delay between the two pump pulses changes. The peak intensity of the signal at the zero delay is -15 times stronger than that at -60ps (pulse B arrives in advance) or at -60ps (pulse A arrives in advance). Its width (FWHM) is about a half of the width at 60ps delay. The observed dependence of the DFWM signal on the relative delay times between the two write beam pulses can be described as follows. The two write-pulses are assumed to have Gaussian temporal distributions with pulse widths  $2\tau_p$  and to cross spatially inside the sample. The intensity of pulse A is expressed as

$$I_A = I_A^0 \exp\left[-\left(\frac{t}{\tau_p}\right)^2\right] \quad (3)$$

where  $t=0$  is defined at the pulse peak. if the time delay between the two write-pulses is  $\Delta t$ , the intensity of pulse B at time  $t$  is therefore written as

$$I_B = I_B^0 \exp\left[-\left(\frac{t + \Delta t/2}{\tau_p}\right)^2\right] \quad (4)$$

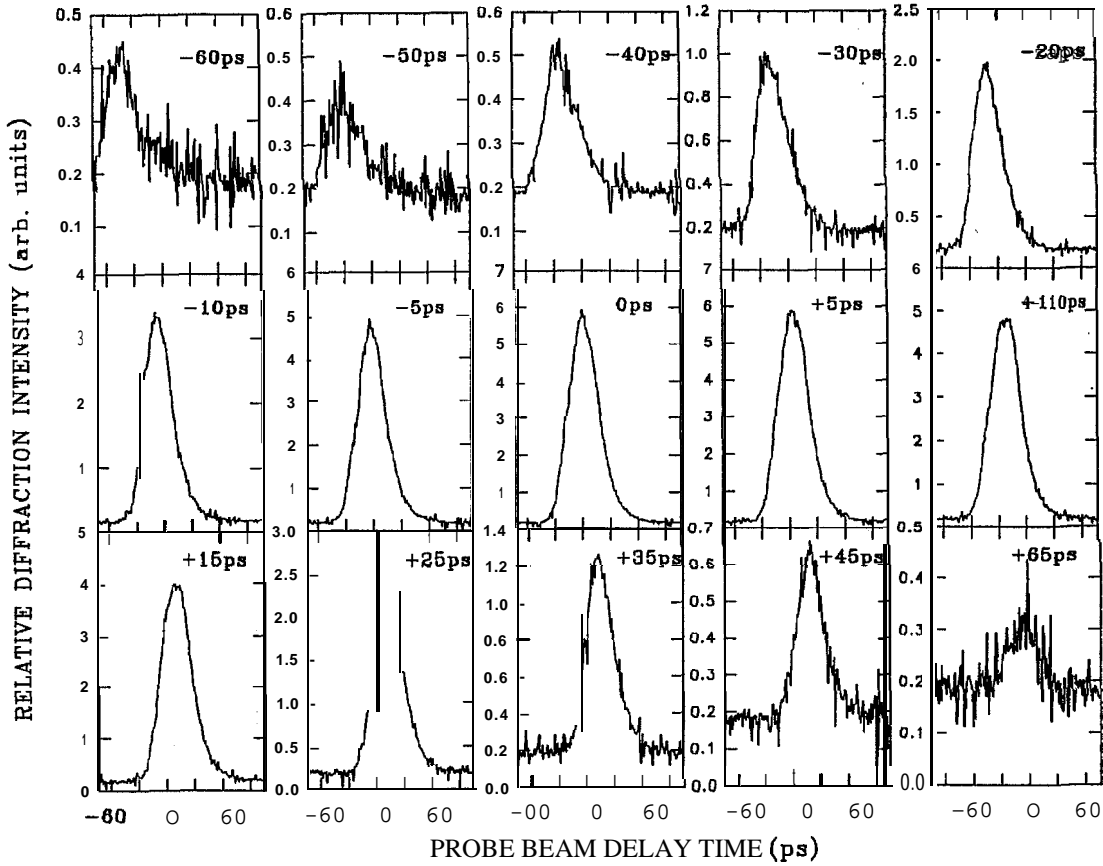


Fig. 3. Diffraction signal intensity as a function of the relative delay between the two pump pulses for CS<sub>2</sub> standard.

The intensity at the peak of the interference pattern between the two write-pulses can be expressed as:

$$I = I_A(t) - I_B(t) + \Delta I \quad (5)$$

where, 
$$\Delta I = A_A A_B \exp[-(\frac{\Delta t}{2\tau_p})^2] \exp[-(\frac{\Delta t}{\tau_p})^2] \quad (6)$$

and  $A_A$ ,  $A_B$  are the magnitudes of the electric fields of the pump beams A and B respectively. Taking  $I_A = I_B$ , the interference intensity is then expressed as

$$I = I_A \{1 + \exp[-(\frac{\Delta t}{2\tau_p})^2] + 2 \exp[-3/2 (\frac{\Delta t}{2\tau_p})^2]\} \quad (7)$$

Using the power-law dependence measured for the diffraction efficiencies of CS<sub>2</sub>,<sup>10</sup> the normalized diffraction intensities versus  $\Delta t$  are found to be in good agreement with Fig.3. Eq.(7) shows how important the fine adjustment of  $\Delta t$  is. If the laser pulse width used in DFWM is in nanosecond range the misalignment  $\Delta t$  of the two write pulses arising from the path difference is not significant. If the pulse width is in picosecond or femtosecond range, however, a little inadvertency may cause a significant discrepancy in  $\chi^3$  measurement.

#### 4. CONCLUSION.

In DFWM measurement of niobate crystals the host excitation caused by two-photon absorption may form small polarons in samples, resulting in a broader, long lived, and slowly decaying signal. Using DFWM in a  $K_x 1 C$  geometry the signal broadening of the coherent response can be eliminated. Regarding to  $\chi^{(3)}$  measurement for different niobate crystals, the pump-pulse adjustment in DFWM measurement is crucial. It can be optimized using a  $CS_2$  reference sample.

#### Acknowledgements

This work is supported in part by NASA under the contract NASA-MURC NCCW-0088 and the U.S. Army Research Office, DAAH04-96-10416.

#### References

- 1) H. Liu, R.C. Powell, and L.A. Boatner, *Phys.Rev.B*, 44 (1991) 2461; 49 (1994) 6323; *Opt. Mater.*, 4 (1995) 691.
- 2) M. Zgonik and P. Gunter, *J. Opt. Soc.Am.B*, 13 (1996) 570.
- 3) N. Sugimoto, H. Kanbara, S. Fujiwara and K. Tanaka, *Opt. Lett.*, 21 (1996) 1637.
- 4) A.E. Bieber, D.F. Prelewitz, T.G. Brown and R.C. Tiberio, *J. Opt. Soc.Am.B*, 13 (1996) 34.
- 5) V.L. Bogdanov and A.G. Spiro, *SPIE Proc.*, 2527 (1995) 275.
- 6) H. Liu, B. Taheri, W. Jia, *Phys.Rev.B*, 49 (1994) 10166.
- 7) W.J. Blau, H. J. Byrne, D. J. Cardin, T. J. Dennis, J. P. Hare, H. W. Kroto, R. Taylor and D. R. M. Walton, *Phys.Rev.Let.*, 67 (1991) 1423.
- 8) Z. H. Kafafi, J. R. Lindle, R. G. S. Pong, F.J. Bartoli, L. J. Lingg and J. Milliken, *Chem.Phys.Let.*, 188 (1992) 492.
- 9) O.F. Schirmer and D. von der Linde, *Appl. Phys. Lett.* 33 (1978) 35.
- 10) M.G. Kuzyk, R.A. Norwood, J.W. Wu, and A.F. Garito, *J. Opt. Soc.Am.B*, 6 (1989) 154.